DesignCon 2014

Sources and Compensation of Skew in Single-Ended and Differential Interconnects

Eben Kunz, Oracle Corp.
Jae Young Choi, Oracle Corp.
Vijay Kunda, Oracle Corp.
Laura Kocubinski, Oracle Corp.
Ying Li, Oracle Corp.
Jason Miller, Oracle Corp.
Gustavo Blando, Oracle Corp.
Istvan Novak, Oracle Corp.

Disclaimer: This presentation does not constitute as an endorsement for any specific product, service, company, or solution.

Abstract

In high-speed signaling with embedded clock a few ps in-pair skew may cause serious signal degradations. Point-to-point topologies, long PCB traces put the emphases on local speed variations due to bends, glass-weave, deterministic and random asymmetries. First we analyze the contributors to the delay in single-ended traces. Length in differential pairs varies due to bends and turns. At each turn the outer trace has a little extra length. We show that using the center-line trace length can give a delay estimation error up to several ps. We will show how different turns, right angle, double 45-degree or arced turn, impact delay. Second, we look at practical ways of compensating skew. A few options are looked at and their performances compared. We consider a few statistical contributors to skew and establish a limit below which compensation makes no sense. The simulated data is illustrated by the measured performance of a few simple structures.

Author(s) Biography

Eben Kunz graduated from MIT in 2012 with a BS and Master's in EE. His thesis project was the design and construction of analog processing components for a low frequency radio telescope. He joined Oracle in May 2012, and has been working on simulation and modeling of high-speed interconnects.

Jae Young Choi is a Hardware Engineer at Oracle Corp. His current work includes high-speed interconnect modeling and simulation, measurement, and characterization. He received his Ph.D. in Electrical and Computer Engineering from the Georgia Institute of Technology.

Vijay Kunda is a Senior Hardware Engineer at Oracle Corporation. He works on modeling and simulation of high speed serial interconnects along with DDR4 memory simulations. His prior work involved full board simulations and timing analysis of DDR2/3/4 memory designs. He received his MS in Electrical Engineering from the University of South Carolina specializing in Antenna Design.

Laura J. Kocubinski is a hardware engineer at Oracle Corp. She currently works on signal integrity within Oracle's SPARC T-Series server division. She recently received her BSEE, with a technical concentration in signal processing, from Rensselaer Polytechnic Institute.

Ying Li is a Hardware Engineer at Oracle Corporation where she works on signal and power integrity of ASIC packaging interconnects simulation and measurement validation. In previous graduate studies, her research work focused on computational electromagnetics, sensitivity analysis and optimization. She received her Masters degree in electrical engineering from McMaster University. She is pursuing her Ph.D. degree at University of Washington.

Jason R. Miller is a Principle Hardware Engineer at Oracle Corporation where he works on ASIC development, ASIC packaging, interconnect modeling and characterization, and system simulation. He has published over 40 technical articles on the topics such as high-speed modeling and simulation and co-authored the book "Frequency-Domain Characterization of Power Distribution Networks" published by Artech House. He received his Ph.D. in electrical engineering from Columbia University.

Gustavo J. Blando is a Principle Hardware Engineer with over ten years of experience in the industry. Currently at Oracle Corporation, he is responsible for the development of new processes and methodologies in the areas of broadband measurement, high speed modeling and system simulations. He received his M.S. from Northeastern University.

Istvan Novak is a Senior Principle Engineer at Oracle. Besides signal integrity design of high-speed serial and parallel buses, he is engaged in the design and characterization of power-distribution networks and packages for mid-range servers. He creates simulation models, and develops measurement techniques for power distribution. Istvan has twenty plus years of experience with high-speed digital, RF, and analog circuit and system design. He is a Fellow of IEEE for his contributions to signal-integrity and RF measurement and simulation methodologies.

I. Introduction and Background

Skew is the deviation of propagation delay from required reference timing. Skew is important in traditional parallel synchronous busses between the data lines of the parallel bus and a separate timing signal. In such cases skew was usually between the transition of the timing signal and the transition of loaded single-ended signals. The main source of skew was the length difference and electrical loading of the devices along the lines and only to a lesser extent the variations of the propagation characteristics of the printed-circuit lines. Beyond a few hundred Mbps, skew has to be reduced by using a forwarded or embedded clock. Because of the embedded clock, in high-speed signaling the lane-to-lane skew has low importance. The differential signaling used in most high-speed serial design, however, requires a tight skew management between the positive and negative legs of a lane. Multi-Gbps data rates may allow only a few ps skew before signal degradation, such as mode conversion, reduction of signal magnitude or EMC problems show up [1], [2], [14], [15]. With point-to-point topologies and long PCB traces, new emphasis must be placed on local variations of the propagation speed due to bends and turns [3], [4], glass-weave effects [5], [6], [7] and similar deterministic and random asymmetries between the positive and negative legs of a differential pair.

Skew is the time-of-arrival error of a signal with respect to some reference time. It is inherently a time domain parameter, relying on the measurement of propagation delay. Whether we measure skew in the time or frequency domain, already the definition of the propagation delay raises questions. When we measure the time of arrival of a waveform, we need both a reference time and a reference level. As *Figure 1* illustrates, as soon as the transition waveforms are not identical in shape at the source and destination points, the (propagation) delay value depends on the reference level we select, introducing further uncertainty.
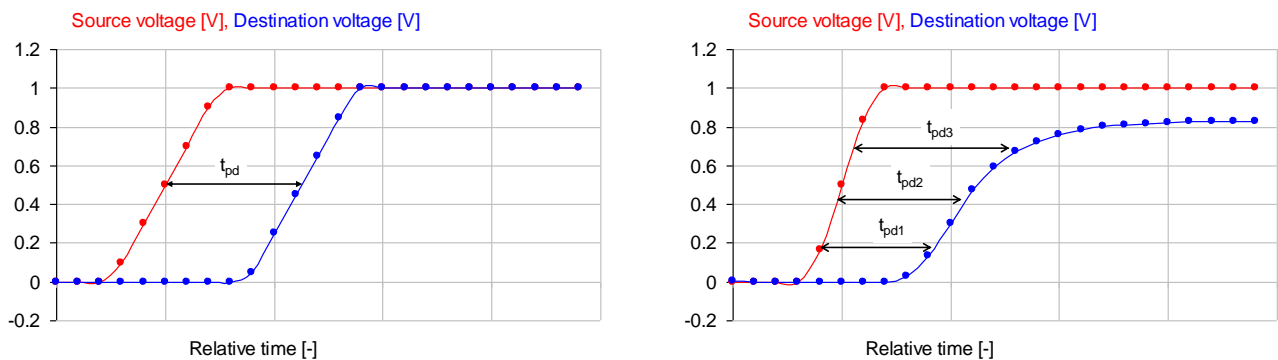
Figure 1: *Illustration of delay definitions with ideal edges (on the left) and with different reference and target waveforms (on the right).*

The selection of reference level becomes important when the signal propagates through a dispersive, lossy media. The signal magnitude and the signal wave shape both will change.

When we measure delay in the frequency domain, we can calculate a phase delay or group delay (the derivative of phase delay) for the reference and target signals, but these delay numbers will be a function of frequency. *Figure 2* illustrates the phase and group delays calculated from causal models of single uniform transmission lines.
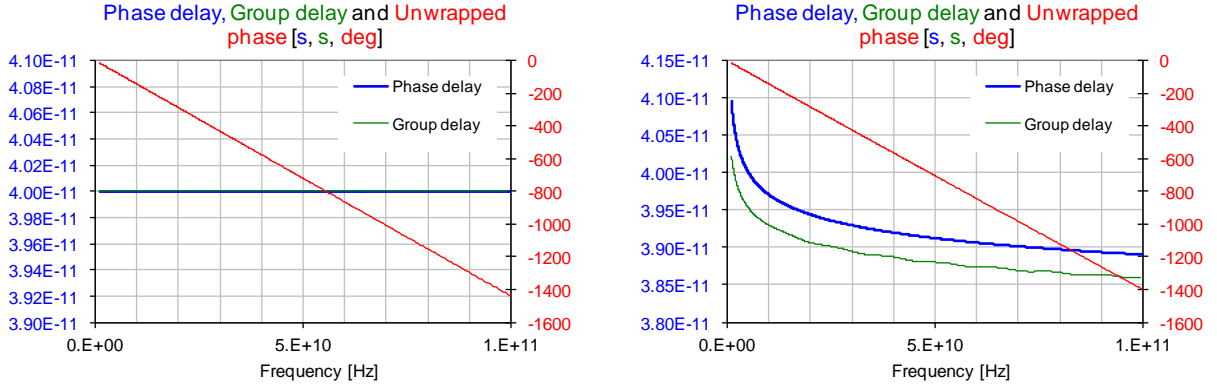
Figure 2: Phase delay and group delay for an ideal 50-ohm uniform transmission line (left) and a causal lossy 50-ohm transmission line of the same length (right).

Note that the phase delay and group delay both decay with increasing frequency, and both are steeper at low frequencies. This behavior is related to the facts that inductance as well as capacitance will go down as frequency goes up and this also means that the group delay line is running below the phase delay line.

$$\gamma(\omega) = \sqrt{(R(f) + j\omega L(f))(G(f) + j\omega C(f))} = \alpha + j\beta = \alpha + j\omega\, t_{pd} \tag{1}$$

$$t_{pd} = \frac{unwrapped\ \_\ phase\ (S_{ji})}{\omega} \tag{2}$$

Data in *Figure 2* assumed matched interconnects, in other words the reference impedance for the scattering matrix equals the characteristic impedance of interconnect. When the reference impedance does not equal the characteristic impedance, the delay values will also depend on reflections, as shown in *Figure 3*. This eventually convolves the effects of locally changing propagation velocity and characteristic impedance [8].
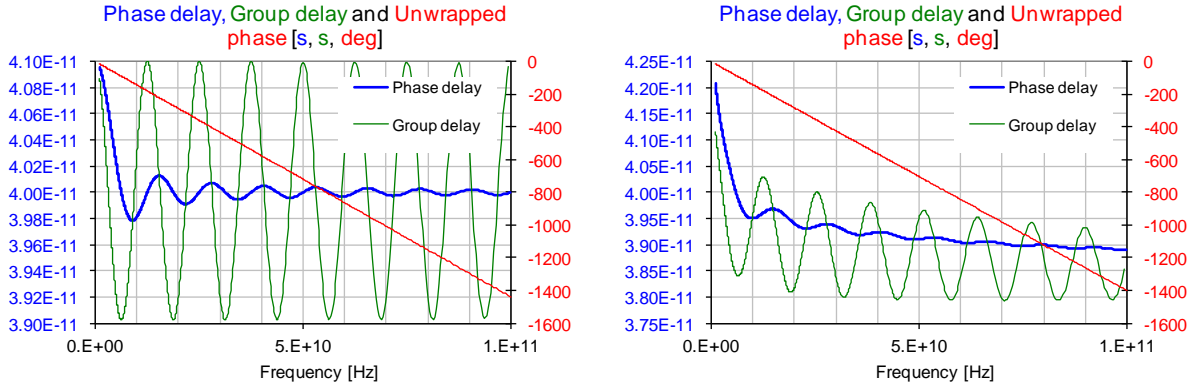
Figure 3: *Phase delay and group delay calculated with 40-ohm reference impedance for an ideal 50-ohm uniform transmission line with 40 ps delay (left) and a causal lossy 50-ohm transmission line of the same length (right).*

When reflections are present, the steady-state (frequency-domain) and transient time-domain delays will be different: while the transient, incident-wave delay remains the same, the steady-state phase and group delays show periodic fluctuation with frequency. The fact that reflections have an effect on steady-state delay suggests that in *Eq. (2)* we should calculate the unwrapped phase from the actual transfer function of interest (say V_{out} / V_{source}) rather than from the *S* parameters, which do not carry information about the source and load reflections. On the plot of *Figure 3* we should notice that both the phase delay and group delay have values lower than the 40 ps delay of the line. A similar trend is seen also on *Figure 4*, but because of the dispersion introduced by losses this effect is not so obvious. With group delay this is less surprising since we know that at resonances it can even go negative. With phase delay, on the other hand, we may suspect that values lower than the ideal propagation delay of the loss less line indicates non-causality.

To understand what is going on, it is useful to look at extreme cases. *Figures 4* and *5* show the same loss less interconnect we had on *Figures 2* and *3*, except we now assume much larger mismatch. The first minimum of phase delay with a 10:1 mismatch is 30.8 ps. With 10,000:1 mismatch the first minimum bottoms out at 20 ps, which is half of the 'normal' 40 ps value. The first minimum occurs at 12.5 GHz, which corresponds to a half-wavelength resonance calculated with the 40 ps delay value. Note that after the 12.5 GHz resonance, the phase delay jumps up to 60 ps and eventually at much higher frequencies it settles at 40 ps. The reason for this large deviation from the expected 40 ps value is explained by the unwrapped phase curve: it is now essentially a staircase starting at -90 degrees. This is happening because the chosen values create an almost perfect integrator. A transmission line terminated in high impedances can be simplified as its static capacitance driven by a current source, which is an integrator circuit with constant phase shift. Though with such extreme termination values we could not practically use the interconnect for

5

signal transmission at frequencies other than narrow bands around the half-wave resonances, this figure illustrates and explains the physical reason why phase delay with mismatches can be lower than matched phase delay.
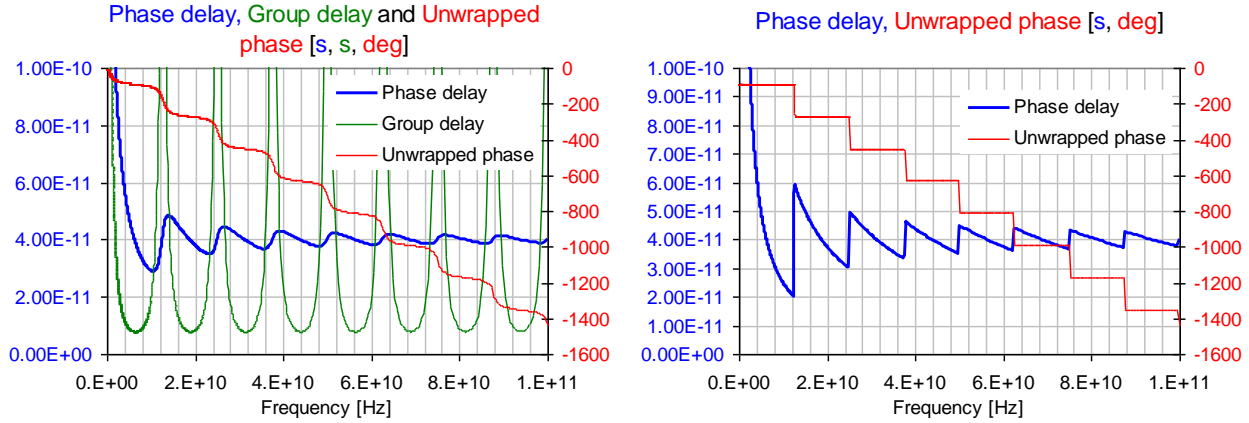
Figures 4 and 5: *Phase delay and group delay calculated with 500-ohm reference impedance (on the left) and 500 kOhm reference impedance (on the right) for an ideal 50-ohm uniform transmission line with 40 ps delay.*

Any asymmetry between positive and negative legs of a differential pair causes a difference in phase delay, which in turn results in signal distortion in the time-domain response. Consider two 12 inches long differential pairs, of which the measured intra-pair difference in phase delay is 3 ps and 18 ps, respectively.
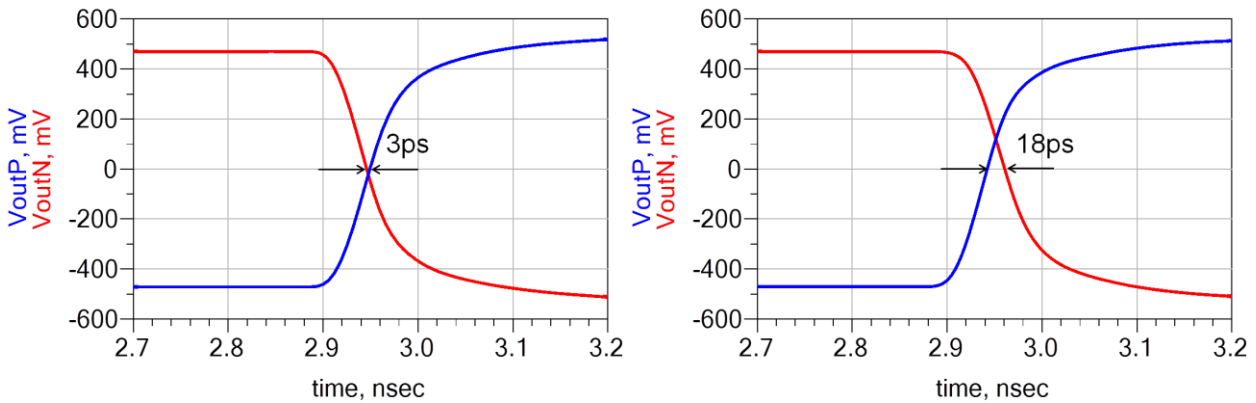
Figure 6: *Distortion created by skew. Output voltages at the receiver show a difference between a board with 3ps (left) and 18ps (right) of skew.*

This differential pair is connected to a differential source, which is defined as a step function transitioning between -500 mV and +500 mV with a rise time of 50 ps. The resulting simulated

waveforms at the receiver are shown in *Figure 6*. Comparing the two figures, the existing intra-pair skew actually shows up in the time-domain response and the skew numbers are well preserved. To further investigate the time-domain response, the rise time of the differential input signal has been swept from 1ps to 100ps. As a result, the resultant skew number for single transient edges stays the same regardless of the rise time, suggesting that the skew can affect the differential signal quality in a wide data-rate range. In contrast, when there are multiple reflections along the signal path, the resulting frequency-dependent phase delay creates rise-time dependent skew.

Geometrically there is a deterministic element of length variations when we route a complex board and need to bend or turn traces several times, which in differential trace pairs will result in a length difference. At each turn the outer trace has a little bit of extra length.

$$l_2 - l_1 = 2*(s + w)$$

$$l_2 - l_1 = 4*(s + w)*\tan(22.5^o) = 1.66*(s + w)$$

$$l_2 - l_1 = 0.5*s*\pi = 1.57*(s + w)$$
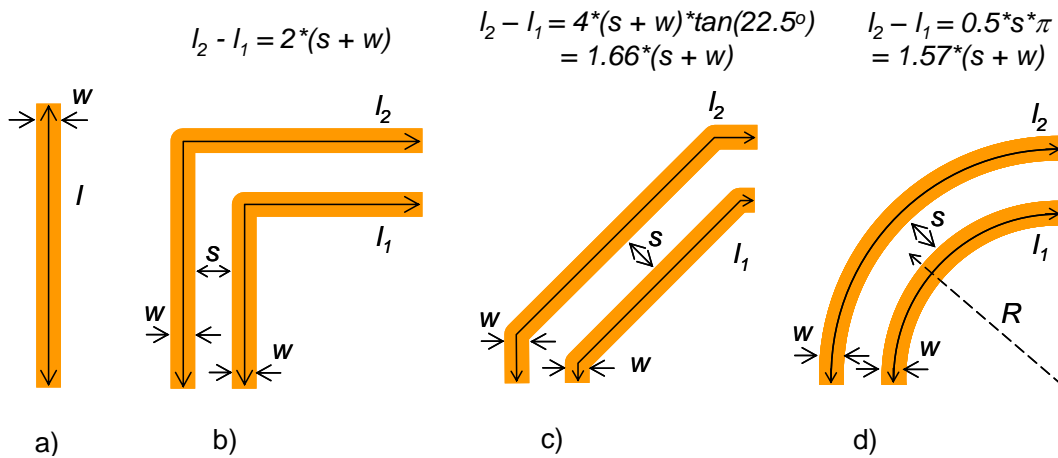
Figure 7: *Center-line length differences of differential pairs based on layout geometry.*

Figure 7 shows the top views of four cases: a) is a straight etch for reference, b), c) and d) are differential pairs making a sharp 90-degree turn, double 45-degree turns and an arced 90-degree turn, respectively. The expression above each sketch shows the center-line length difference. We will look at these structures again in more detail in later sections.

To determine the extra length in the outer traces of a pair, we face an important question: what is the length of a trace with bends and turns. No matter how narrow traces we use, the inner perimeter of the turning shape is always shorter than the outer perimeter. Not knowing better, we may use the centerline length of each trace. If we assume $w = s = 6$ mils and $t_{pd} = 150$ ps/", we get 24-mil, 19.9-mil and 18.8-mil center-line difference and 3.6 ps, 2.99 ps and 2.82 ps calculated skew for cases b), c) and d), respectively. Note that for all three geometries, the length difference is proportional to the sum of trace width and trace separation, suggesting that in general, narrower and tighter coupled traces at bends incur less skew.

Still deterministic, but somewhat harder to quantify is the change of delay at bends and turns due to the resulting discontinuities. Discontinuities of this sort are small localized fields, which we may be

7

approximated as small lumped capacitive or inductive loads at the location of the turns. The reactive loading changes the overall propagation delay and it also changes the impedance of the trace. The changing impedance creates reflections, which also has an impact on the delay. The bends and turns in this respect are somewhat similar to vias, which are vertical right-angle turns with additional features (pads and antipads), potentially creating more discontinuities and variations of the propagation delay. And finally there are a number of statistical effects contributing to the uncertainty of the delay. Part-to-part and layer-to-layer variations of the dielectric constant due to glass-weave effects and due to the slower potential variations of glass-resin ratio along the area of the board.

II. Layout and Material Dependent Skew

In the Introduction we looked at the obvious and deterministic skew sources, such as center-line length difference and impedance mismatches. In this section we will look at skew contributors due to statistical weave effect, current redistribution and via-stub differences.

II. 1. Skew due to current redistribution

We will start looking at skew by analyzing the various contributors to the propagation delay in single-ended and differential traces. The total propagation delay in homogeneous matched and lossless interconnects is the product of the signal path length and propagation velocity. On a real printed circuit board, there are several factors that complicate the evaluation of this product. In today's dense printed circuit boards we usually assume that the trace width and dielectric layer height are much smaller than the wavelength of our signals. While this may be true, when we need to calculate propagation delay and skew to the ps level, we cannot ignore the finite trace width. The delay will be proportional to the effective path length of the signal, and the trace (and return-plane) cross sections allow significant redistribution of current at different frequencies. A 6-mil trace width in a typical PCB laminate environment represents approximately 1 ps delay perpendicular to the main direction of signal propagation, which suggests that even if the center-line length is perfectly on target, just the current redistribution differences may cause this much of 'uncertainty' in the delay.
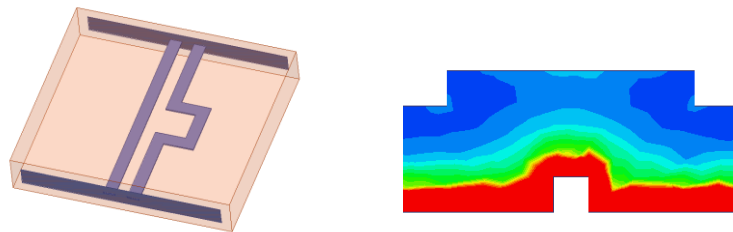
Figure 8: Illustrating the frequency dependent shortcut path around trace corners. Differential pair CAD geometry on the left, current distribution in the compensation trace on the right.

8

This is illustrated in *Figure 8*, showing the current distribution in a rectangular delay-correction element. Note that the current does not follow the center-line path of the trace, and not only because of the proximity effect from the other trace.

II. 2. Skew due to via-stub asymmetry

Asymmetric back-drilling of vias can create a source of skew. Consider a differential pair of vias consisting of 68mil long via barrel, trace-out pads, and via stubs as shown in *Figure 9*. The stubs are remaining via barrel sections that the back-drilling process cannot remove. Their lengths may vary randomly within the manufacturing tolerance. Because any asymmetries may cause skew, asymmetric stubs in a differential pair can also be a source of skew. Note that in this case there is no difference in the signal-path length between the two legs; any skew is the result of asymmetry in reflection.

To quantify the skew generated by asymmetric via stubs, a parametric study was conducted using 3D field solver by varying the via stub lengths, creating seven different cases as shown in *Table I*.

Table I.

Case	P stub (mil)	N stub (mil)
1	0	0
2	6	6
3	6	10
4	6	15
5	10	10
6	10	15
7	15	15
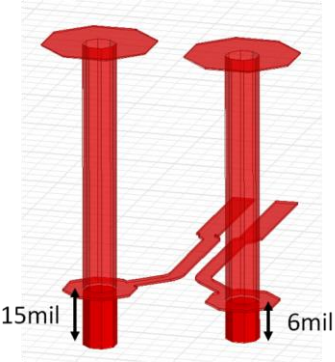
Figure 9: Asymmetric stub lengths

Figure 10 shows the simulated loss profiles. Although the difference is small, losses are characterized more by the length of the longer stub than by asymmetry. However, the mode conversion curves shown on the left in *Figure 10* indicate that the asymmetric stub lengths increase

9

more differential signal converted to common mode signal. In addition, the calculated differential skew values on the right in *Figure 11* show that the maximally asymmetric stubs can add more than 1ps of skew at 14 GHz and above. Although the stub length asymmetry may introduce larger skew, the stub length variation is less likely happen within a single board.
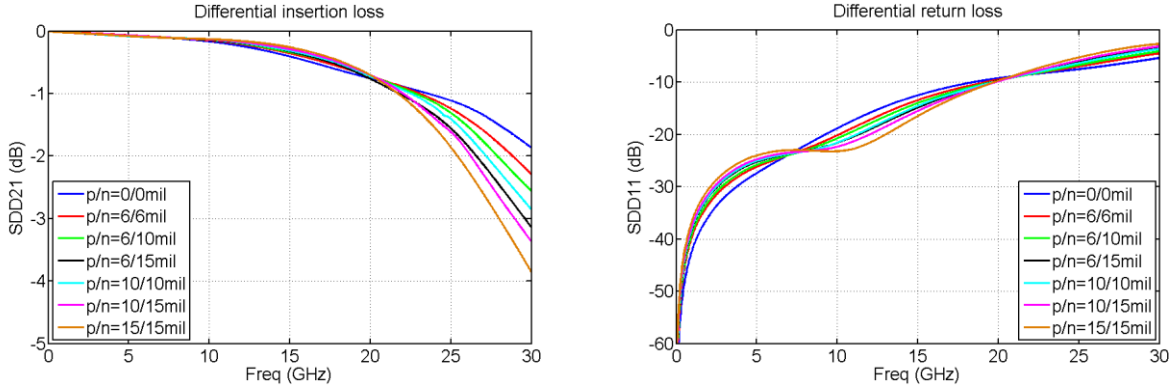
Figure 10: Differential insertion loss (left) and return loss (right).
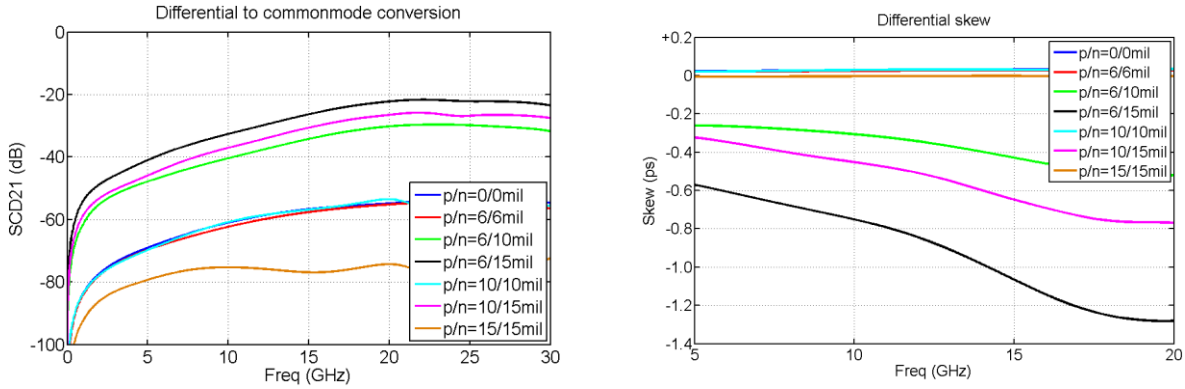
Figure 11: Differential to common mode conversion (left) and differential skew (right).

II. 3. Skew due to glass weave

The dielectric materials used to build printed circuit boards comprise of resin/epoxy and glass weave. The electrical properties of resin and glass weave are different and this leads to inhomogeneous environment although the actual dielectric is treated as homogeneous. The glass weaves are combinations of fills and warps interweaved. The fiberglass has certain pitch and spacing between fills/warps depending on the type of material. Due to limitation in PCB manufacturing, these weaves do not always align well with the traces. This is a concern for differential signaling since the weave-trace alignment may not be same for each leg of the differential pair. This increase

10

common mode conversion and differential skew. We will examine the impact of asymmetrical trace-weave alignment on skew.
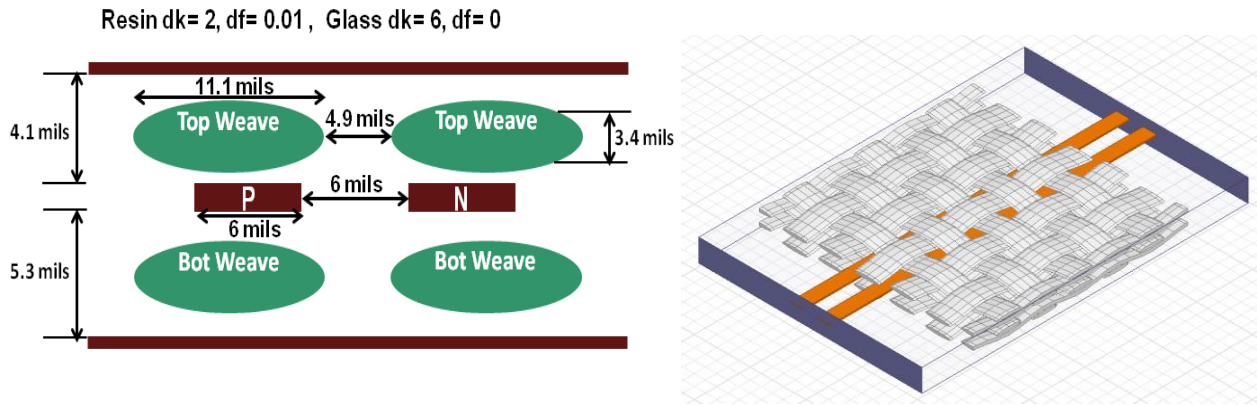
Figure 12: *Geometrical description of the stripline structure with 3313 1-ply glass weave on top and bottom of the trace (left), 3D CAD stripline structure [10] with 3313 glass weave (on right)*

Figure 12 shows a 96 mil stripline with 3313 glass bundles on both top and bottom of the trace along with resin and the 3D CAD structure [10] used for simulation. The pitch of the 3313 glass is approximately 16 mils and is 3.4 mils thick in this example. The S-parameters are concatenated to understand the skew for 6 inches of stripline. The differential traces are symmetric if both legs are perfectly symmetric with respect to weave. Due to PCB variation, the P trace may be completely under the weave and the N trace could be partially under the fill/warp separation.

Figure 13 (left) shows how the differential skew varies for the 6 inch trace as the traces are offset to weave. In all of these simulations, for simplicity, the top and bottom weaves are assumed to move together. In reality, these may be independent variables and the skew could be reduced. This assumption is explored further in Section II.3. When the offset is 0/8/16 mils, the P and N are very close to being symmetric. Similarly, they are fairly asymmetric when the offset is 4/12 mils.
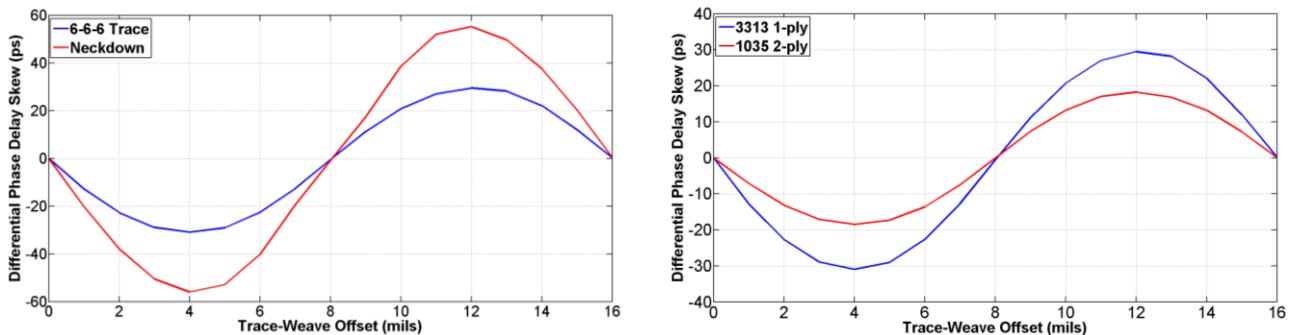
Figure 13: *Impact of trace - 3313weave offset on differential skew for regular and neck down traces for 6 inches of stripline(on the left), Comparison of the differential skew between 3313 1-ply and 1035 2-ply due to trace-weave offset for 6 inches of stripline.*

The worst case skew due to these non-alignments could increase significantly. For a regular 6-6-6mil 6 inch differential signal the worst case skew is around 30 ps, which is 5 ps/inch. The skew changes with offset because each trace sees a different dielectric combination. For a neck down trace of 4.2-3.2-4.2 mil, the worst case skew increases to 9 ps / inch. The skew for the neck down is greater due to thinner traces which makes the differential signaling even more asymmetric.

One way to minimize the skew is to use a different glass material that is less thick that has tighter pitch and by using 2-ply instead of a single ply. The thinner glass material reduces the impact on skew as the traces are exposed to less weave even when the traces are asymmetric. Two-ply material may help to reduce skew further due to the glass bundles spreading out horizontally. We ignore this potential benefit here but simply the thickness reduction (going to a 2-ply 1035 with 1.1 mil per ply thickness) reduces the skew compared to single ply. The reduction in differential skew compared to 3313 1-ply glass can be seen in *Figure 13* (right) as the trace-weave offset changes in 1 mil increments. For the same 6 inches of stripline, the worst case skew is reduced from 5 ps/inch to 3ps/inch.

PCB manufacturing limitations can also lead to the traces not running parallel to the weave. Instead, the weave is at a certain angle to the trace. This angle will also have an impact on skew. *Figure 14* shows how skew varies when the weave angle with respect to the trace changes from 0 degrees to 45 degrees. The plot on the left shows the skew variation when the trace to weave offset is 0 mils and we observe the skew does not change significantly with the angle. But when the trace weave offset is 4 mils (on the right), a small change in the angle can lower the skew significantly. One important observation here is that for small trace-to-weave angles (few degrees from zero) the skew is not significantly reduced. Beyond that, we see significant benefit from insuring the weave is rotated with respect to trace. The nulls observed occur when there is a balance of glass density across the differential pair as the glass is rotated.
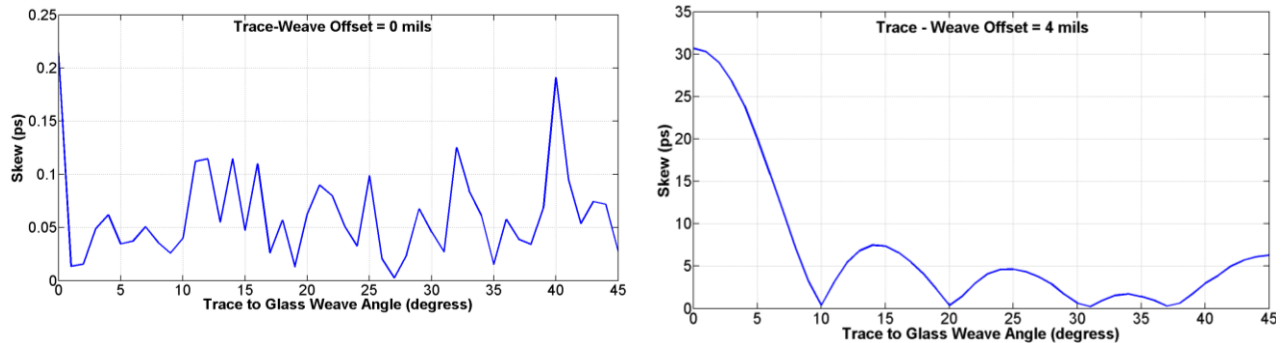
Figure 14: *Impact of trace - 3313weave angle on skew for regular trace of 6 inches of stripline when the offset is 0 mils (on the left), and when the offset is 4 mils (on the right).*

One of the major consequences of skew are resonances which are caused by the phase rotation [13]. As the skew increases the fundamental resonance frequency is pulled lower and as a result these resonances could fall within the operating speeds of some of the SERDES links. *Figure 15* shows the differential insertion loss for a 50 Ohm 10 inch neck-down stripline as the trace-weave offset varies from 0 to 16 mils.
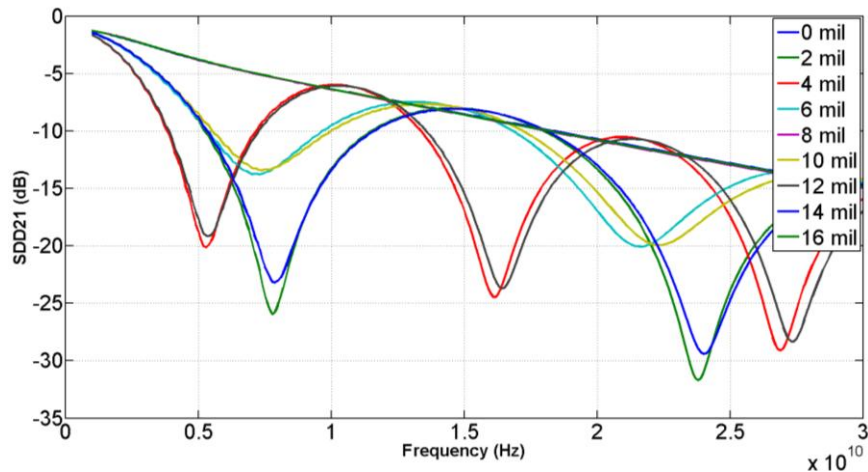
Figure 15: *Skew resonances due to trace-3313 1-ply weave offset for 10 inches of stripline*

When the traces are offset by 0/8/16 mils, there is no resonance but for other cases there are resonances at odd harmonics. These resonances can easily be calculated from the difference in electrical length from skew. The worst case skew is around 9 ps/inch when the offset is 4/12 mils and this corresponds to resonance at the 1st harmonic of 5.5 GHz.

III. SKEW COMPENSATION

One of the sources of skew is the length difference between positive and negative legs of a differential pair.

III. 1. Compensation with rectangular bulge on one leg

As briefly discussed in the introduction, current redistribution effects in delay structures can cause skew to be underestimated. In this section we explore this phenomenon further. *Figure 16* (left) is the calculated skew error on differential pair with a rectangular bulge on one leg, used for skew compensation. The skew error is defined here as the difference between the calculated skew, using the center line distance, and the phase delays. We observe that the skew error is less sensitive to the length of the bulge but quite sensitive to offset since small offsets allows current to "scoot" around the bulge, reducing the added skew.

Figure 16 (right) plots the same data as *Figure 16* (left) except with the actual skew values on the Z-axis. By keeping both plots in mind, we see that if we calculate skew based on the center line distance we can, for example, compensate for 3 ps of skew with a only 30% error; on the other extreme if we try to compensate for ~1 ps of skew, we may incur unacceptably high skew error using the center line distance. The challenges with using larger skew compensation structures is a) introduction of an increasing asymmetric discontinuity and b) a large skew correction threshold (i.e., in this example we can't correct for much less than 3 ps without incurring a lot of skew error).   The answer to this dilemma is to of course simulate each rectangular bulge (or equivalent structure) to

13

accurately predict the skew compensation. However, even this approach has its own minimum skew correction threshold due to elements of the simulation environment that might not be captured such as the glass weave.
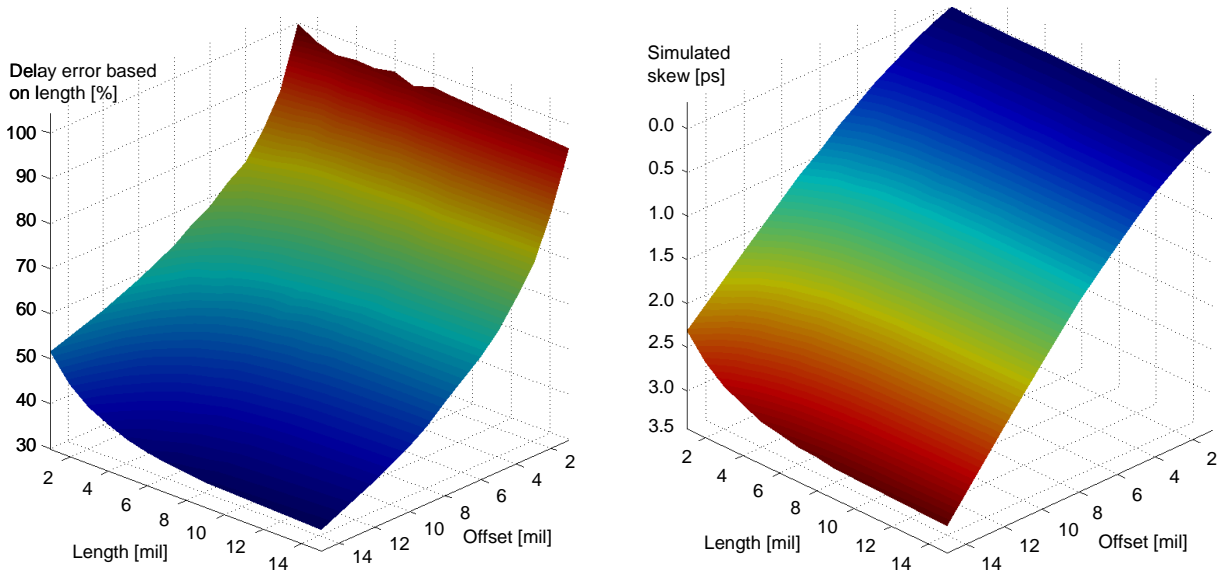
Figure 16: *Calculated percentage skew error (on the left) and magnitude skew error (on the right) of a differential pair with a rectangular bulge on one leg, used for skew compensation.*

III.2. Compensation by opposite turns

A conventional way of compensating the skew created by the length difference is to place another source of skew but with opposite signature. For example, in *Figure 17*, a differential stripline pair makes a 90-degree clockwise turn consisting of two 45-degree turns, resulting in one leg to be physically longer than the other. This length asymmetry is subsequently compensated by another 90-degree counter-clockwise turn followed by a straight trace with length L. As a result, the simulated skew is nearly zero (<0.05 ps).
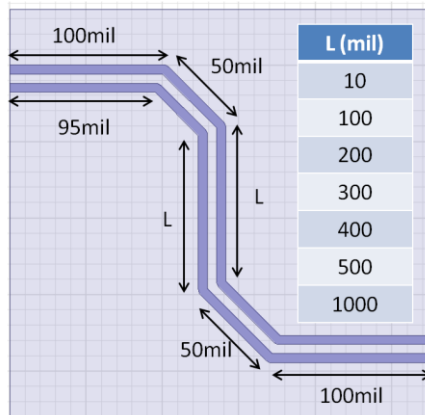
Figure 17*: Differential pair with two 45-degree bends and the compensation bends.*

To determine the optimal location of the compensation bend and how the efficiency of compensation changes, the length L has been varied from 10mil to 1000mil. The resulting mode conversion curves are shown in *Figure 18*; the compensation efficiency does not significantly change with the location of the compensation bend although we do observe the mode conversion increasing with the length L. This result can be understood by the fact that the propagation speed of differential and common-mode signal in differential stripline is the same. On the contrary, if the speeds of the two propagation modes are different, e.g. a microstrip, the location of the compensation bend will significantly affect the quality of skew compensation [9].
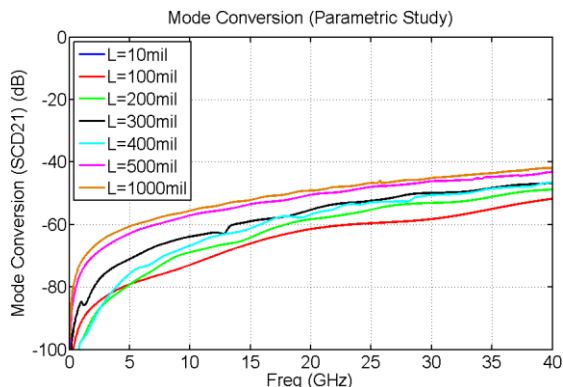
Figure 18: *Differential to common mode conversion as spaces between trace bends changes.*

Consider a 100mil-long differential pair which needs to turn 90 degrees clockwise. To make a right-angle turn, either a circular bend or two turns of 45-degree bends can be used as shown on the left and right in *Figure 19*, respectively. The total etch lengths, measurement of a hypothetical center line between two legs, are 250.03 mil for 45-degree bends and 258.63mil for the arc.
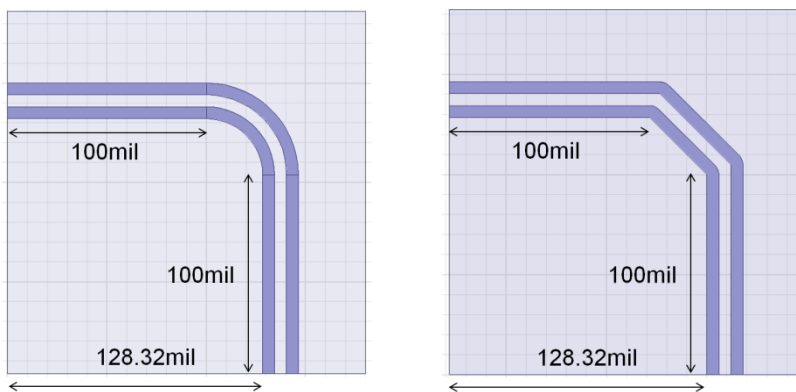
Figure 19: *Two types of trace bends. An arc (left) and 45-degree bends (right).*

The two bends were simulated and the resulting differential insertion and return loss curves are shown in *Figure 20*.
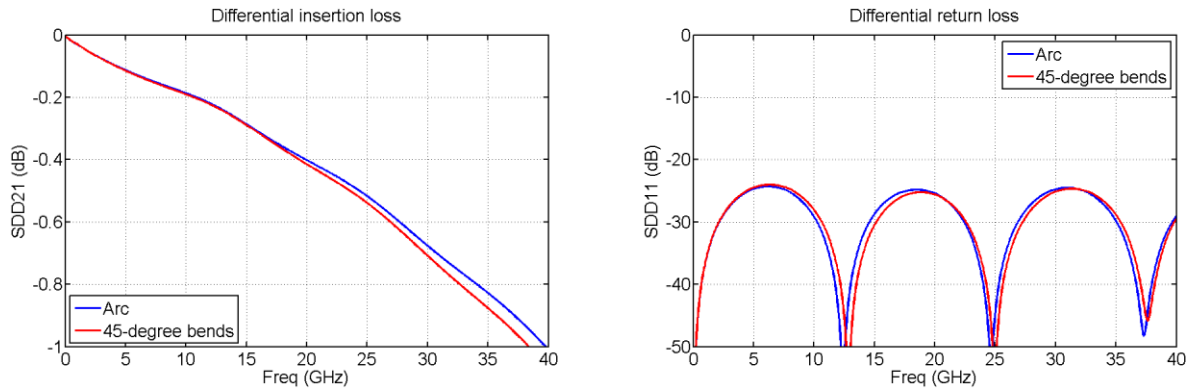
Figure 20: *Differential insertion and return loss.*

The 45-degree bends have slightly more insertion loss while return loss are similar for both types of bends. Notice that the arc is 8.6mil longer, but shows less insertion loss.
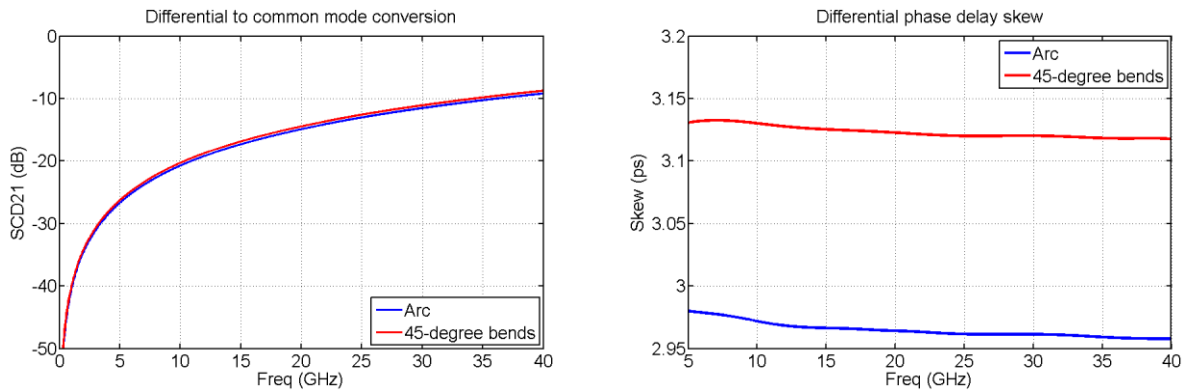
Figure 21: *Differential to common mode conversion (left) and differential skew (right).*
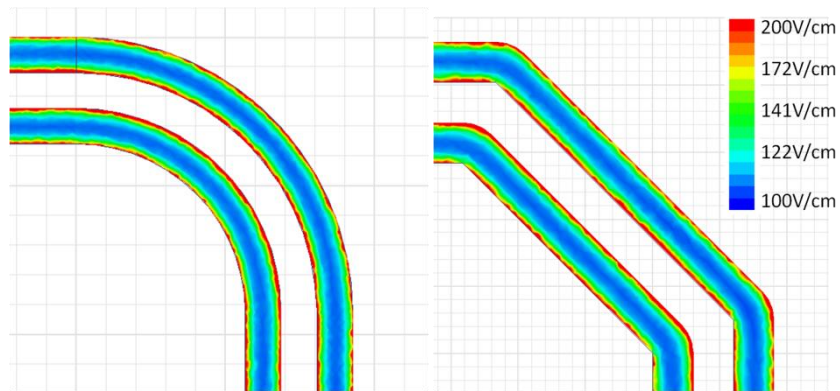
Figure 22: *Surface current density at the different types of bends –arc (left) and double 45-degree (right).*

16

The mode conversion is shown on the left in *Figure 21*, and the 45-degree bends convert differential signal to common mode about 0.45 dB more at 20 GHz. The differential skew, shown on the right of the figure, also indicates that the 45-degree bends add about 0.06ps more than an arc. These skew numbers compare relatively well with skew based on center-line length differences that we calculated in the numerical example at *Figure 7*. Other than the 5% shorter center-line difference of the arc, the 45-degree bends and round arcs perform similarly in the frequency range up to 20 GHz.

Surface current density plots at the two bends have been generated and shown in *Figure 22*. We can observe slightly higher current density during the tern along the facing edges of the traces: the current redistribution tends to lengthen the current path on the inner trace and shorten it in the outer trace, thus reducing skew.

III. 3. Statistical treatment of weave generated skew

It has been well established that glass weave can create skew within differential pairs [11]. There is reasonable evidence that the angle between glass weave and PCB panel edge is variable within some limits [5]. This analysis uses a statistical model that approximates the effect of one or more layers of glass weave, taking into account the angle variability of each layer. No data was available about how weave angle varies across a PCB, or how often different layers might naturally align with each other, so an independent truncated Gaussian distribution was assumed for each layer's weave angle. Unlike a true Gaussian distribution, there should be some angle beyond which the weave mechanically cannot be placed.
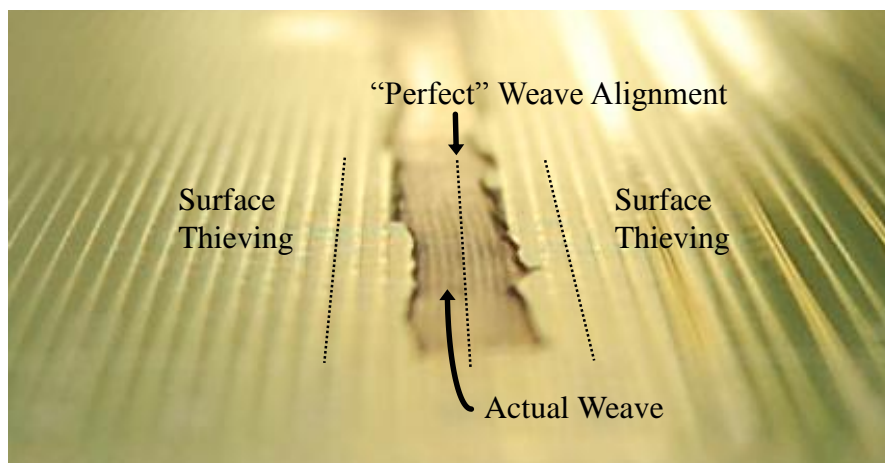
Figure 23: A partially milled PCB with weave that turns relative to surface thieving / panel edge. Image is taken at a shallow angle for contrast.

As a starting point, a 64 mil section of weakly coupled differential etch was simulated within a realistic PCB containing four layers of weave: two in the prepreg (A,B), and two in the core (C,D). See *Figure 7* for a similar simulation with only two layers of weave. Weave was aligned with the etch, and parameterized to vary each weave offset (y_A, y_B, y_C, y_D) along an axis perpendicular to the

etch. The weave structure was generated with a 16 mil bundle pitch, and each layer was offset independently by 0, 2, 4, 6, and 8 mils, for a total of 625 combinations.

Due to time constraints, and because resonance from neighboring weave bundles perpendicular to the etch only becomes a factor at very high frequencies (~100 GHz+), only a single frequency was simulated. Resonance and skew from weave bundles nearly parallel to the etch are not considered, since it is infeasible to account for in the analysis that follows. 10 GHz was selected as a low enough frequency that phase does not wrap, but high enough that low frequency effects are negligible (e.g. skin depth model breakdown). This skew value is taken to be representative of the wideband performance of the differential etch.
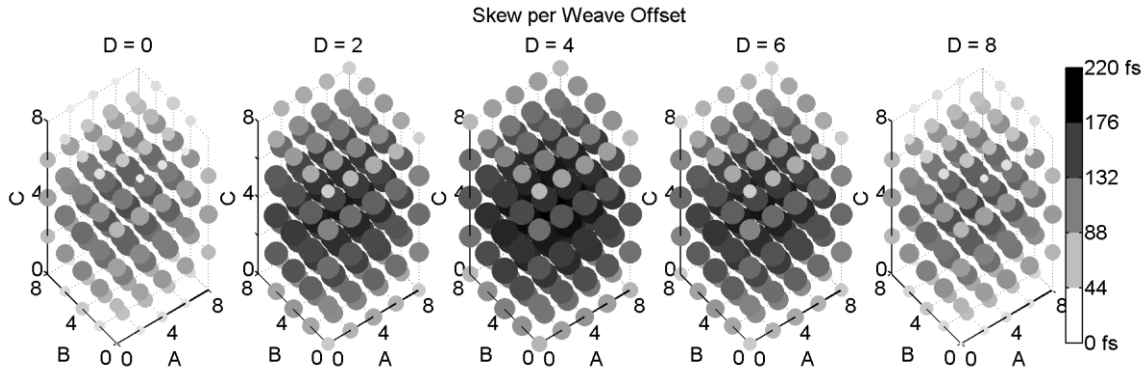
Figure 24: *Skew at 10 GHz for 64 mils of differential etch, varied by weave offsets (A-D, mils).*

In order to get the most accurate skew value, each simulation was converted into an S parameter and renormalized at each port independently to reduce return loss. This minimizes any skew caused by asymmetric port reflection, which would not appear in reality since weave must vary continuously. The resulting data shows that skew caused by offsetting different layers is largely independent, so each layer's skew $S(y)$ can be fitted to a sine function independently of others. Since each layer is independent, the offsets from 8 to 16 mils are assumed to be a continuation of the sine curve by mechanical symmetry (See *Figure 7*). This also means that skew can be analyzed for each layer independently, vastly simplifying further analysis. The maximum fitting error for all 4 layers combined is 8 fs / 64 mils, with a maximum simulated skew value of 217 fs / 64 mils. The maximum skew observed for symmetrical combinations (only 0 or 8 mil offsets) is 4.6 fs / 64 mils, so the fitting error is within the realm of simulation error.

$$S_N = k_N \sin(y_N \cdot 2\pi/16) \tag{3}$$

$$S(y_A, y_B, y_C, y_D) = S_A(y_A) + S_B(y_B) + S_C(y_C) + S_D(y_D) \tag{4}$$

$$k_A = 0.438\ ps/in \quad k_B = 0.625\ ps/in \quad k_C = 0.938\ ps/in \quad k_D = 1.25\ ps/in$$

With skew for short sections of etch established, skew for longer sections of etch can be calculated by adding the skew from discrete short sections. Weave angle is approximated by gradually shifting the weave offset as if the weave were actually angled. Skew addition works because the etch is very weakly coupled, so changes in skew due to crosstalk are negligible. This analysis does not include

changes in wave length along the etch, and breaks down when weave angle is sufficiently steep to affect bundle spacing. For angles less than $10°$, error is limited to ~1.5%. As a reference, each constant k is also the worst case skew generated by that layer.

A single layer skew function $S(y)$ is combined with a probability distribution function (PDF) of weave angle, $P(\theta)$, which provides a probability for each angle the weave could be placed at. Eventually this produces a PDF of skew $P_X(s)$ for each distance x along a piece of etch. Discretization is necessary if arbitrary weave angle PDFs must be handled in the future. Etch runs from $x = 0$ in steps of $\Delta x = 16$ mils. For each segment of etch, weave offset y is in discrete steps. It is assumed that the likelihood of each y offset is equal at any point along x. Skew is also discretized. $P(\theta)$ is remapped to generate a PDF of weave offset across Δx of $P_{\Delta x}(\Delta y)$, using $\sin^{-1}$ instead of $\tan^{-1}$ to be consistent with the weave angle approximation.

$$P_{\Delta x}(\Delta y) = P\left(\theta = \sin^{-1}\frac{\Delta y}{\Delta x}\right) \tag{5}$$

For each x and y value, a discrete PDF of skew values $P_{X,Y}(s)$ is created. Skew PDFs for the same x value are combined into a matrix $M_X(y, s)$, which is renormalized to a sum of 1 for convenience. For $x = 0$, skew is 0 with probability 1. Subsequent matrices $M_X(y, s)$ are computed by first adjusting for the appropriate $S(y)$ at each y, then convolving with $P_{\Delta x}(\Delta y)$ along the y axis at each s. This approximates a weave which contributes a small amount of skew, then changes y offset based on angle. Finally, $P_X(s)$ is calculated by summing $M_X(y, s)$ over y.

$$M_{X=x+\Delta x}(y, s) = \sum_{\Delta y} M_{X=x}(y - \Delta y, s + S(y - \Delta y) \cdot \Delta x) \cdot P_{\Delta x}(\Delta y) \tag{6}$$

$$P_X(s) = \sum_y M_X(y, s) \tag{7}$$
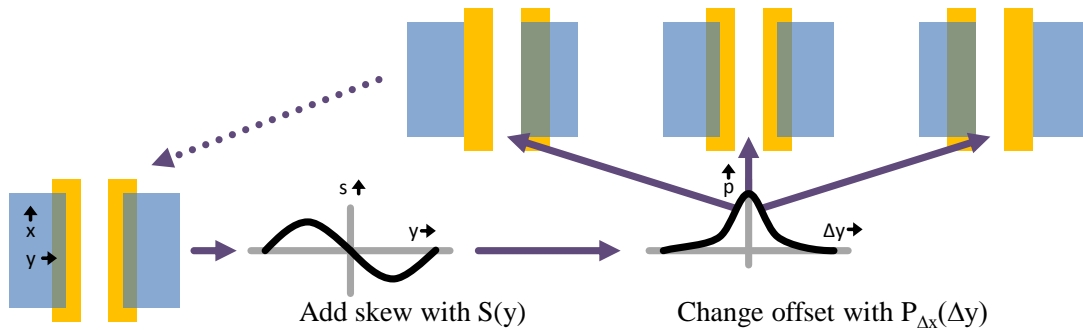
Figure 25: *Steps for iteratively generating skew probabilities.*

$P_X(s)$ can be used to generate useful metrics of weave performance, including mean $\mu(x)$ and standard deviation $\sigma(x)$ for skew. To start with, weave layer B, and the associated $S_B(y_B)$, is used in isolation as a demonstration. With $k_B = 0.625$ ps/in, the worst case skew is 0.625 ps/in. Below are four sets of $P_X(s)$, varied by μ and σ of the $P(\theta)$ Gaussian. These cases are selected to show trends, and are only loosely based on observed weave. The skew axis is adjusted to show average

skew per inch up to each length, which aids visualization. As etch length increases, variability in weave angle tends to partially correct skew. If weave bundles are on top of both halves of the differential pair for equal fractions of total etch length, the net amount of skew would be zero, which is increasingly likely as total length increases. Most notable in these cases, even a slight change of weave angle mean from zero results in a significant reduction in expected skew per unit length.
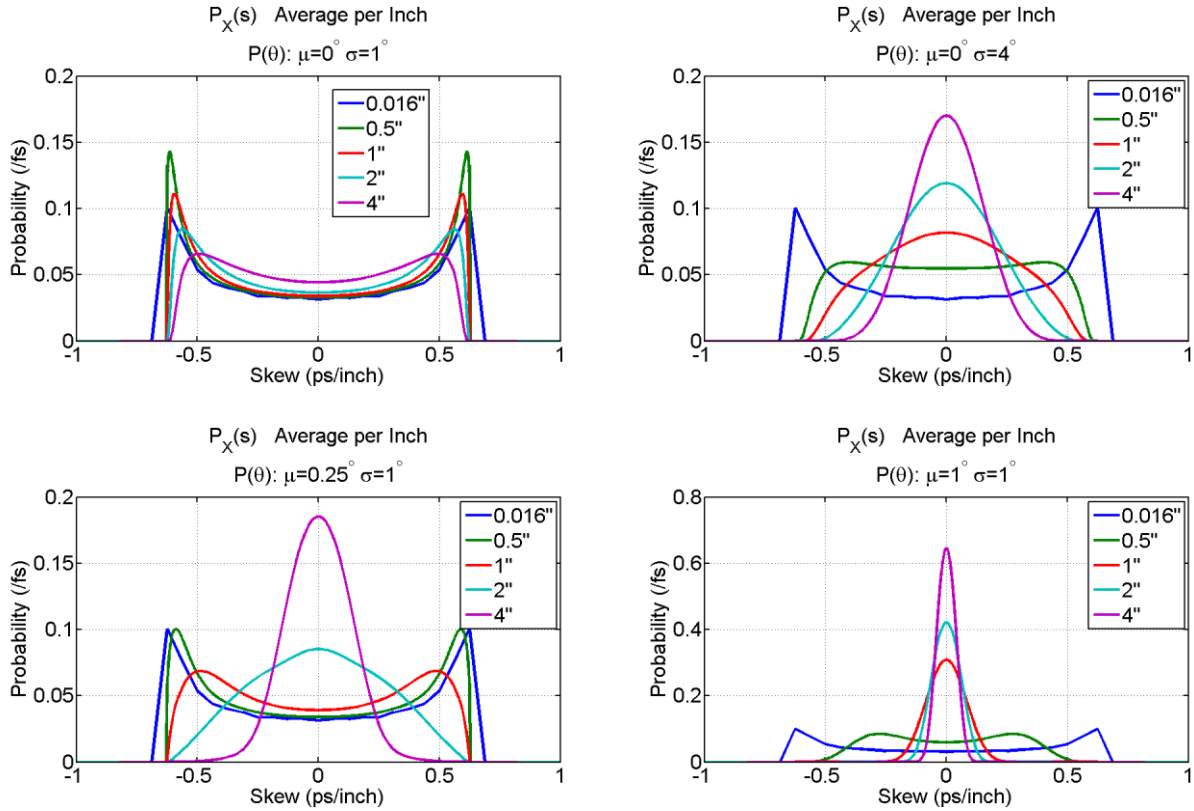
Figure 26: *Skew PDFs for various weave angle PDFs.*
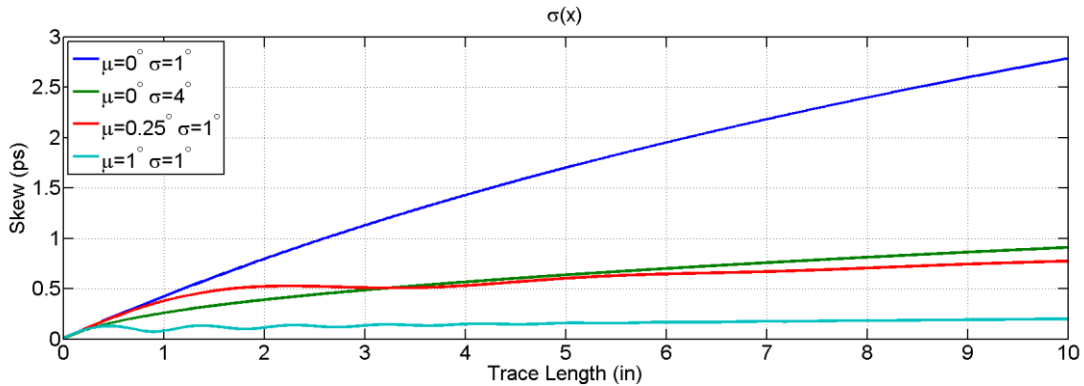
Figure 27: *Skew standard deviation for various weave angle PDFs.*

For the same four cases, $\sigma(x)$ provides additional insight into skew behavior. Skew is usually taken as an absolute value, and expected absolute skew tracks $\sigma(x)$ closely. With non-zero mean angle, as the weave crosses the etch, skew tends to oscillate with a spatial frequency proportional to weave angle. For even small angles, $\sigma(x)$ levels off as etch length increases, especially when the weave is fairly straight. This is a good indicator that the model is representing physical behavior properly. Because $P_X(s)$ is not Gaussian, especially for small x, and changes shape with x, making statements of skew likelihood based on multiples of σ is not useful. More useful is to pick a failure rate, here $P = 10^{-3}$ or 0.1%, which is the number of traces or PCBs that are "bad", and are presumably discarded. A CDF is used to calculate the maximum amount of expected skew for the remaining "good" traces/PCBs. In cases where the PDF is wide and flat, expected skew at $P = 10^{-3}$ is very close to the worst case of 6.25 ps at 10". When the mean angle reaches 1°, expected skew levels off below 1 ps. As the failure rate is reduced (not shown), the 1° weave maintains an expected skew below 1 ps. The failure rate may apply to whole PCBs, or to individual etch, depending on how consistent weave is across a single PCB.
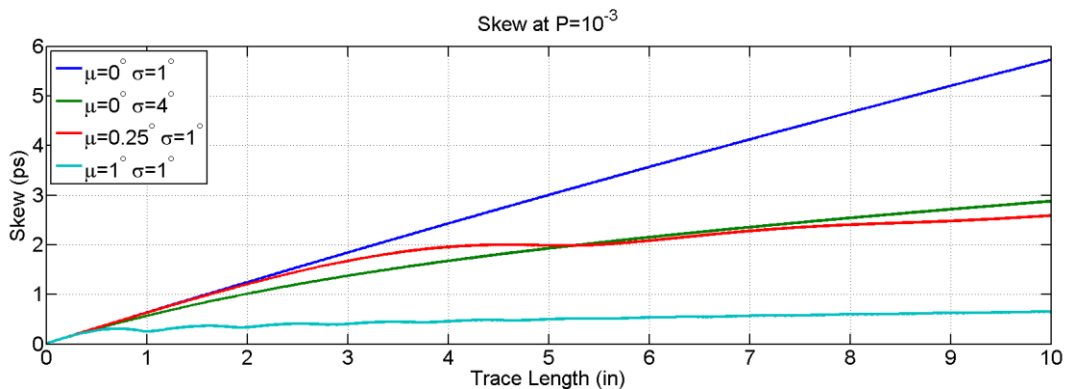
Figure 28: Skew at a failure threshold for a single weave layer.
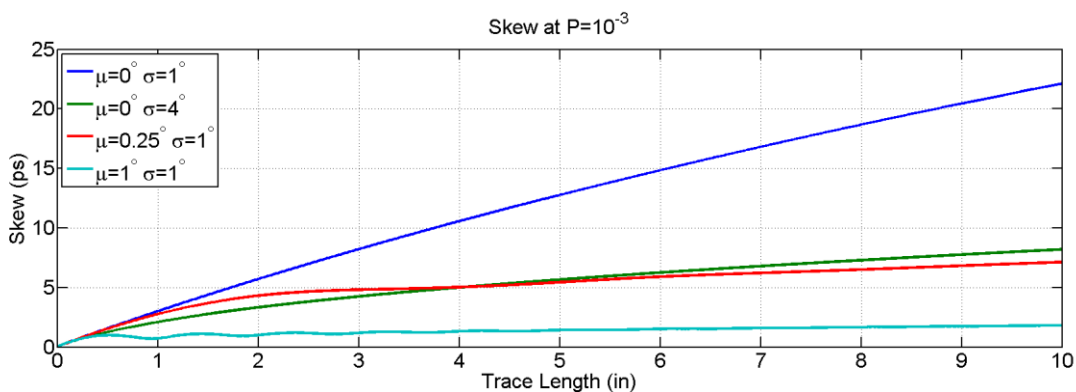
Figure 29: Skew at a failure threshold for four weave layers.

When the skew for all four layers of weave is combined, expected skew at $P = 10^{-3}$ increases, but is a slightly smaller fraction of the combined worst case skew (3.25 ps/in). This is due to the

21

likelihood that different layers will offset each other's skew. The shape of $P_X(s)$ for all four layers (not shown) is much closer to Gaussian, even for small x, so individual $P_X(s)$ are less useful to observe. This is a model of totally independent weave, so if adjacent layers tend to offset by a fixed amount (~6-10 mils), skew would be significantly reduced.

This model can be used to correlate EM simulations of weave with measurement, given sufficient angle data, or to correlate angle data given good simulations of weave. The statistical distribution of a set of skew measurements can be compared to $P_X(s)$, and if correlation is good, the model can be used to inform improvements in skew. It is important to note that this analysis is targeted towards expected behavior, not worst case. The only way to reduce worst case skew is to limit the maximum length along which the weave is perfectly parallel to the etch. How to guarantee that limit, and whether it is necessary, is subject to the specific details of actual weave angle performance and manufacturing. This model does not account for how reflections caused by discontinuities affect weave skew, so behavior may be different when trace bends or vias are introduced.

If this model holds up to measurement correlation, it provides several insights:
1) The ratio of skew per unit length is not as useful as separate skew and length data, especially for weave with a mean angle.
2) Even very small mean weave angles may significantly reduce skew in traces longer than ~500 mils by gradually shifting the weave, which corrects some skew. Note that for traces shorter than 500 mils, weave shifting is limited, so results correspond to those shown in Section II.3.
3) Much more data about weave angle is necessary if the goal is to predict and reduce weave generated skew.

IV. Measurement Data

Electrical performance of a 12" long differential pair has been measured using a 50 GHz 4-port VNA. The measurement was performed using the same measurement instrument and calibration setup for three sample printed circuit boards from a single manufacturer. The measured differential insertion loss curves are shown in Figure 30, and a huge deviation is observed in *Sample 2*; a large dip at 25-30GHz pulls down the whole curve.
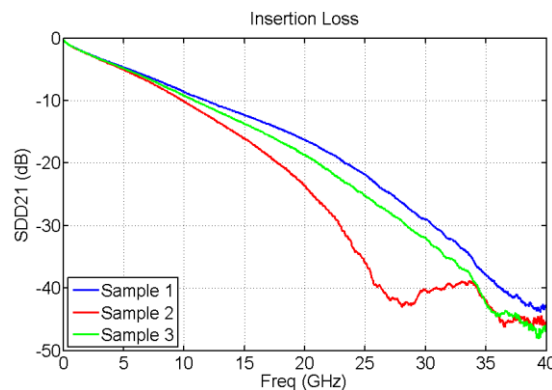
Figure 30: *Differential insertion loss*
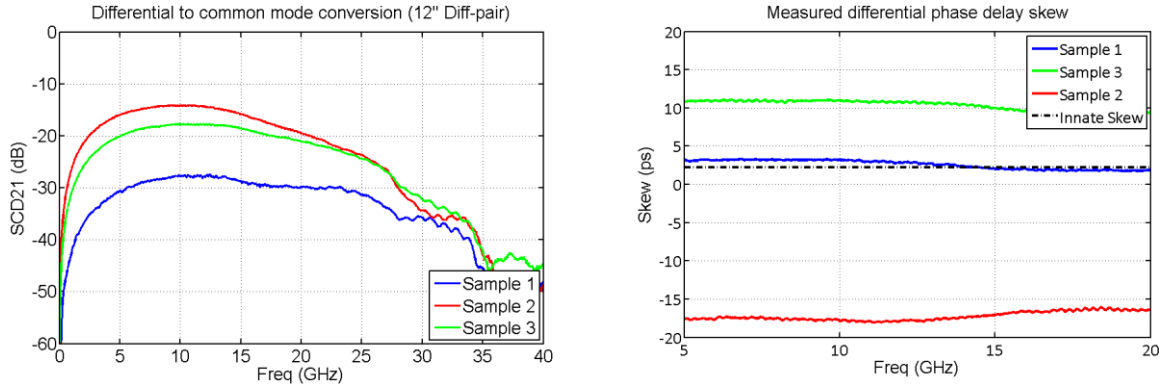
Figure 31: *Mode conversion (left) and differential skew (right).*

As shown on the left in *Figure 31*, mode conversion of *Sample 2* is also very large compared to that of *Sample 1*. Moreover, the differential skew of *Sample 2* reaches up to -18ps, while that of *Sample 1* almost lines up with the expected, layout-based skew, which is basically created by the trace length difference in design (shown by the dashed line on the right in *Figure 31*).

To investigate the source of the skew, the measurement S-parameters of Sample 1 and 2 are converted to TDR as shown in *Figure 32*. Between 0.6ns and 2.5ns, a large impedance deviation between positive and negative legs is observed in Sample 2, whereas Sample 1 shows fairly similar impedance for both legs. Interestingly, the location of the 0.6 ns and 2.5 ns in TDR response corresponds to a 6"-long straight path, parallel to the board edge, in the actual board. This suggests that straight etch (relative to board edge) may be more susceptible to glass-weave inhomogeneities and asymmetries.
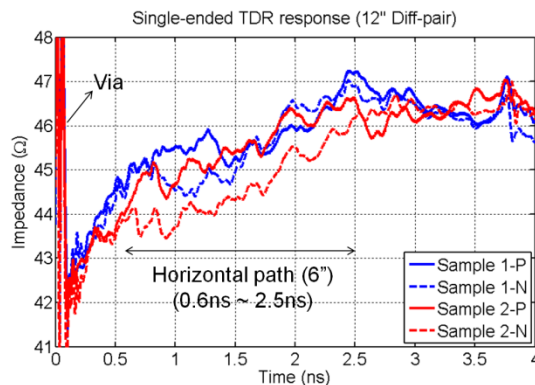
Figure 32: *Calculated TDR response shows P/N impedance deviation.*

To verify that the skew is mainly due to glass-resin combination, measurements were taken of a differential stripline embedded in a non-reinforced homogenous laminate used for packaging substrates. The measurement system was calibrated up to the end of the coaxial cables using an electronic calibration module. The measurements taken with an electronic calibration ideally

23

removes any systematic (time-invariant) errors caused by the imperfections of the test setup and test equipment. Random errors, not accounted for in calibration, may still be introduced.

Two sources of random error associated with the test setup have been quantified in a short study. These sources of error are caused by coaxial cable movement and connector non-repeatability. Ten repeated measurements were taken of the aforementioned test structure; the same electronic calibration was applied to all measurements. Between measurements, the DUT was disconnected and reconnected to the cables, and the cables were oriented differently. *Figure 33* shows that the differential phase delay skew measurements may range from about 0ps to 0.4 ps due to random error.

Figure 34 shows the geometry of the differential stripline. The stripline has a differential impedance of 100 Ohms and is 100 mm long. The dielectric has no glass weave. Both legs of the differential stripline are length matched. Four port VNA measurements show (see *Figure 33)* that the differential phase delay skew is very small (0.2 ps), much less than the peak skew due to random errors. This skew amounts to only 0.05 ps/", much less than what we typically observe from reinforced PCB laminates.
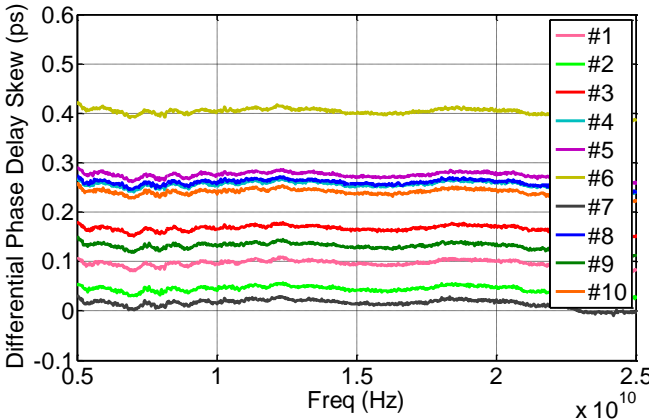
Figure 33: *Differential phase delay skew error associated with cable movement and connector non-repeatability*
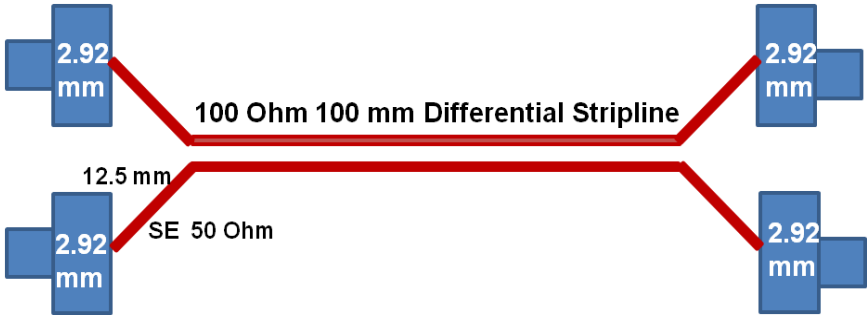
Figure 34: *Geometry of the stripline surrounded by non-reinforced substrate.*
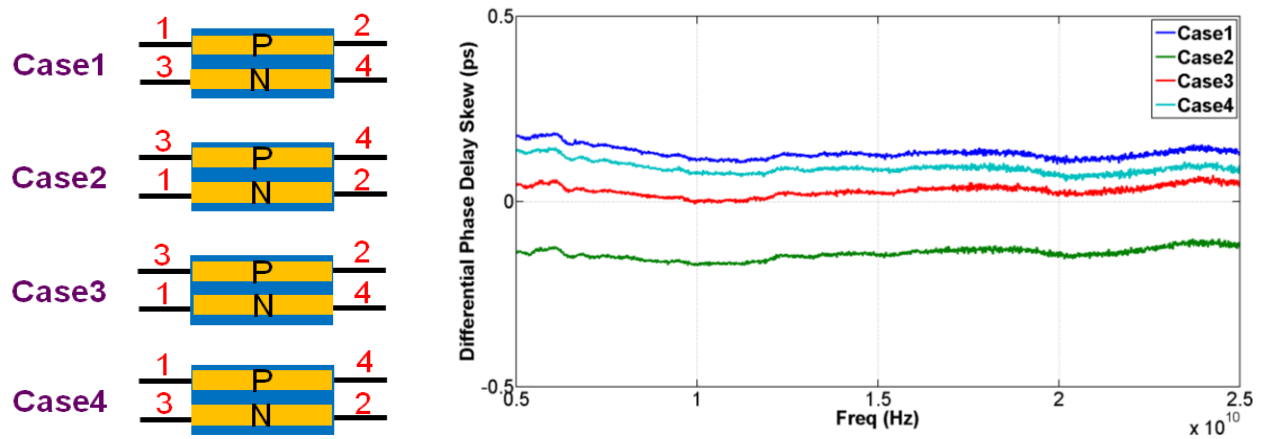
Figure 35: Four cases of VNA measurements (left) and skew plots (right)

Further insight can be gained by measuring the DUT with different VNA port combinations. The skew will follow the ports if it is due to the actual board and not from calibration error. *Figure 35* shows four different cases of port combinations and the differential phase delay skew for all the four cases. It can clearly be understood that the skew is coming from the board as the polarity of skew is reversed when ports for P and N are reversed.

Conclusions

Various contributors to delay variations and skew have been looked at in the paper. The basic definition of delay and skew already needs scrutiny: the commonly used phase-delay definition, based on the corresponding transfer element of the scattering matrix, does not take the reflections at the source and load into account. When accounted for, these reflections create a periodical ripple in the phase delay frequency curve. Current redistribution horizontally within a 6-mil wide trace may account for up to one ps delay uncertainty. 'Corner-hugging' in the current path can introduce up to about three ps skew-compensation error in rectangular skew-compensation structures. Deterministic contributors of skew, such as center-line length difference in differential bends of three shapes were compared. It was found that the center-line length difference in all three geometries is proportional to the sum of trace width and trace separation, biggest in right-angle bends and smallest is rounded arcs. Glass-weave effect was analyzed with full-wave 3D field solver in deterministic worst case and statistical contributions from four identical, but independently positioned and angled glass fabrics. It was found that the worst-case skew introduced by glass weave is proportional to trace length, varies periodically with horizontal offset, and up to a couple of degrees of weave or trace rotation the worst-case skew does not improve noticeably. The statistical analysis on the other hand showed that the expected typical skew drops rapidly with trace length and weave angle. Measured data confirmed the expectation that uniform straight traces in laminates without glass weave do not incur skew. Finally repeated measurements on the same DUT showed that with today's common instrumentation the skew error floor of a differential measurement is a fraction of a ps.

25

VNA measurements showed that the board to board skew distribution of realistic board topologies/routes can be broad and the peak measured skew was quite significant. Post processing of the TDR data suggested that long routes parallel to the board edge may be particularly susceptible to skew variation due to the glass weave.

Acknowledgement

References

[1] V. Seetharam, Michael Brosnan, "Effect of Skew and Rise Time-Fall Time Asymmetry on PCB Emissions," proceedings of 2013 IEEE EMC Symposium

[2] Alma Jaze1, Bruce Archambeault, Sam Connor, "Differential Mode to Common Mode Conversion on Differential Signal Vias due to Asymmetric GND Via Configurations," proceedings of 2013 IEEE EMC Symposium

[3] Chang, et al., "Bended Differential Transmission Line Using Compensation Inductance for Common-Mode Noise Suppression," IEEE Transaction on Components, Packaging and Manufacturing Technology, September 2012

[4] Yuriy Shlepnev, "Design Insights from Electromagnetic Analysis of Interconnects," Front Range Signal Integrity Seminar, Longmont, CO, October 3, 2013

[5] Jason R. Miller, et al., "Additional Trace Losses due to Glass-Weave Periodic Loading," DesignCon 2010

[6] Mykola Chernobryvko, Dries Vande Ginste and Dani¨el De Zutter, "A Perturbation Technique to Analyze the Influence of Fiber Weave Effects on Differential Signaling," EPEPS 2013 proceedings

[7] Gerardo Romo Luevano, Jaemin Shin and Timothy Michalka, "Practical Investigations of Fiber Weave Effects on High-Speed Interfaces," proceedings of 2013 ECTC

[8] Novak, et al, "Determining PCB Trace Impedance by TDR: Challenges and Possible Solutions," proceedings of DesignCon 2013

[9] M. R. Buford, P.A. Levin, and T. J. Kazmierski, "Temporal skew and mode conversion management in differential pairs to 15GHz," IEEE Electronics Letters, Vol. 44, No. 1, 2008.

[10] Chris Herrick, Thomas Buck, and Ruihua Ding. "Simulation Fiber Weave Effect". (http://pcdandf.com/cms/magazine/95/6187), Printed Circuit Design and Fab, May 2009.

[11] Scott McMorrow, Chris Heard, "The Impact of PCB Laminate Weave on the Electrical Performance of Differential Signaling at Multi-Gigabit Data Rates," DesignCon 2005, Santa Clara, CA.

[12] H. Lee, Joungho Kim, "Unit Cell Approach to Full-Wave Analysis of Meander Delay Line Using FDTD Periodic Structure Modeling Method," Proc. IEEE AdvP, vol.25, No.2, May 2002

[13] Gustavo Blando, et al., "Losses Induced by Asymmetry in Differential Transmission Lines," DesignCon 2007

[14] Peter J. Pupalaikis, "Group Delay and its Impact on Serial Data Transmission and Testing," Proceedings of DesignCon 2006

[15] Hung-Chuan Chen, Samuel Connor, Tzong-Lin Wu, and Bruce Archambeault, "The Effect of Various Skew Compensation Strategies on Mode Conversion and Radiation from High-Speed Connectors," proceedings of 2013 IEEE EMC Symposium